Journal of GeoEngineering, Vol. 11, No. 2, pp. 59-73, August 2016
http://dx.doi.org/10.6310/jog.2016.11(2).2

SHEAR STRENGTH EVALUATION OF BENTONITE STABILISED WITH RECYCLED MATERIALS

Umair Hasan [1], Amin Chegenizadeh [2*], Mochamad Arief Budihardjo [3], and Hamid Nikraz [4]

ABSTRACT

The volumetric deviations in montmorillonite-rich clays like bentonite render such soils unsuitable to support overlying pavement and foundation structures. Moreover, green construction and sustainable waste management practices have adapted use of waste recycled materials for engineering purposes. This study explores the feasibility of using recycled construction and demolition waste and ground granulated blast furnace slag for developing shear strength properties of bentonite clay. Direct shear tests were performed on specimens from bentonite and bentonite-stabiliser composites to evaluate the effect of both stabilisers under different curing times and percentages. Microanalyses were conducted to obtain microstructural, mineralogical and elemental composition of the stabilised and unstabilised samples. Results exhibit that shear strength increased with increasing stabiliser percentages and curing time, and the effects were more enhanced on higher stabiliser dosages and curing periods. Sample cohesion value increased from 58.90 kPa for pure bentonite sample to 67.26 kPa for the maximum additive percentages of 5% slag and 20% construction waste (sample S3G5), after 28 days of curing. The internal friction angle also increased by 7.3° from the pure sample to the S3G5 bentonite-stabilisers composite specimen. Peak shear stress values also showed a development of 55.95 kPa after additive induction and 28 days curing, for 200 kPa of normal stress. Curing period also affected the development of cohesion and peak shear strength of the stabilised samples. Internal frictional angle for sample S3G5 also escalated by 2.3°, after 28 days, from the 25.0° value after sample curing of 1 day. Scanning Electron Microscopy (SEM) micrographs and Energy Dispersive Spectroscopy (EDS) spectra show that stabilisers occupied vesicles and cracks found in construction waste particles, resulting in better particle interlocking mechanism and greater shear strength.

Key words: Shear strength, bentonite, recycled materials.

1. INTRODUCTION

Construction project sites are often deemed problematic from a geotechnical and pavement engineering perspective due to the occurrence of weak soils. Many of these soils exhibit swelling-shrinkage cycles triggered by the wetting-drying cycles and are termed as "expansive" or "reactive" soils (Karunarathne *et al*. 2012; Fredlund 2006; Hasan *et al*. 2015). Due to the volumetric fluctuations of such soils, the overlying pavements and foundations are susceptible to failure. The morphological and mineralogical compositions of any type of soil dictate its behaviour. Clays, such as bentonite, fall within the group of soils that can entrap significant volumes of water between molecular sheets depending upon climatic and environmental variations. Reactive clays such as bentonite mainly contains of very fine Na-montmorillonite particles with large surface area that increases their ability to depict volume changes due to higher surface area being exposed for reactions.

Manuscript received January 7, 2016; revised April 4, 2016; accepted May 17, 2016.
[1] Graduate, Department of Civil Engineering, Faculty of Science and Engineering, Curtin University, Perth, Australia.
[2] Researcher (corresponding author), Ph.D., Department of Civil Engineering, Faculty of Science and Engineering, Curtin University, Perth, Australia (e-mail: amin.chegenizadeh@curtin. edu.au).
[3] Lecturer, Ph.D., Department of Environmental Engineering, Diponegoro University, Indonesia.
[4] Professor, Department of Civil Engineering, Faculty of Science and Engineering, Curtin University, Perth, Australia.

The successful application of a suitable soil treatment, commonly termed as soil stabilisation, can help to reduce the degree of soil deformation and the damages to the overlaying structures can be kept within an acceptable range. Soil stabilisation is classified based upon the mode of application such as thermal stabilisation by heating to decrease repulsive forces between clay particles and/or temperatures exceeding 100°C reduced the absorbed moisture volume, either can cause an increase in the soil's strength (Venkatramaiah 2006); mechanical; electrical and stabilisation through nanomaterials such as adding carbon nanotubes. Among other methods, mechanical and chemical stabilisation methods are the most common techniques.

In the wake of green constructions and utilisation of industrial wastes, ground granulated blast furnace slag (GGBFS) has gained wide attention due to its comparatively lower cost and ease of replacing at least part of Portland cement in building and road constructions. GGBFS are the by-product of the steel and iron production industries and have similar characteristics to the rocks produced from vjolcanic eruptions such as granites and basalts, with some hydraulic and cementitious properties. The primary constituents of GGBFS are therefore, lime and other bases silicates and alumino-silicates (Barnett *et al*. 2006; McGrath *et al*. 2014). GGBFS, when activated with lime, is commonly employed in ready-mix concrete or blended cement. Lime either as an additive or as a hydration product of Portland cement, activated the GGBFS to produced improved concrete. The GGBFS-cement concrete has higher impermeability, lower hydration heat, higher resistance against sulphate attack and im-

proved long-term strength (Oss 2003; Ouf 2001). Table 1, reproduced from (Australasian (Iron & Steel) Slag Association 2013), outlines the typical chemical composition of blast furnace slag produced in the Australasian region.

On the other hand, population growth and real estate boom have fashioned need for modernised structures triggering unprecedented volumes of construction waste and demolition from construction of new structures and demolition of older structures. The term construction and demolition waste is generally very broad that may constitute of waste materials such as glass, contaminated soils, asbestos, metals, papers and cardboards, plastics, bricks, asphalt, concrete, rubber and tyres *etc*. from several types of construction activities.

One of the commonly encountered parameters in the study of soil stability is the shearing resistance or shear strength of soil and is primarily used to evaluate the efficiency of stabilisation process in enhancing the soil's capability to resist lateral load that tends to trigger shear failure in the material. For the purpose of this research study, direct shear test was employed. The output data that can be obtained from DST has been summarised in the Fig. 1.

This study is part of an ongoing research on various soil stabilisation techniques in Curtin University (Amiralian *et al.* 2015; Budihardjo *et al*. 2015(a), 2015(b)). It is an extension of an earlier experimental work performed by Hasan *et al.* (2016) employing both chemical and mechanical soil stabilisation methods.

Table 1 Typical composition of Australasian GGBFS (ASA 2013)

Constituent	Symbol	Percentage (%)
Calcium Oxide	CaO	41
Silicon Dioxide	SiO_2	35
Aluminium Oxide	Al_2O_3	14
Magnesium Oxide	MgO	6.5
Titanium Oxide	TiO_2	1.0
Iron Oxide	Fe_2O_3	0.7
Sulphur	S	0.6
Manganese Oxide	MnO	0.5
Potassium Oxide	K_2O	0.3
Vanadium Oxide	V_2O_5	< 0.05
Chromium Oxide	Cr_2O_3	< 0.005

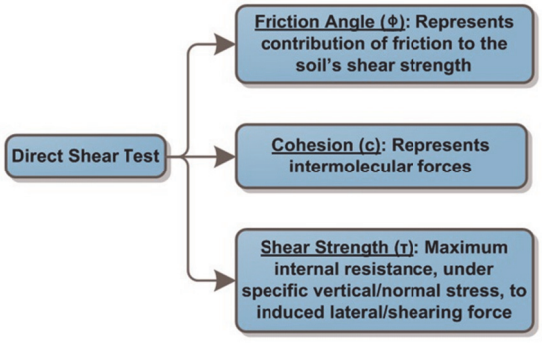

Fig. 1 Typical parametric outcomes of direct shear test

Chemical additive stabilisation was performed by adding controlled volumes of GGBFS, whereas mechanical stabilisation was performed through adding construction waste (CW). The compressive strength of the composites was studied in the previous study, whereas this study investigates the shear strength parameters. Therefore, several elemental and geotechnical characterisation tests were performed to study the morphology, microstructure, and direct shear strengths of the stabilised and unstabilised samples.

2. MATERIAL AND METHODOLOGY

2.1 Test Design

The efficiency of the adapted two additive materials; namely construction waste (CW) and ground granulated blast furnace slag (GGBFS) in enhancing the mechanical characteristics of the reactive soil was evaluated through laboratory experiments. Direct shear strengths of the stabilised and unstabilised specimens were calculated and the possibility of morphological and mineralogical changes within the soil matrices was also explored. The outline of the research work is produced in the flowchart illustrated in Fig. 2.

2.2 Materials and Sample Preparation

Commercially manufactured bentonite was used in this study to investigate the shear strength enhancement of montmorillonite-rich expansive clay as has also been investigated by other researchers (Abdelrahman *et al.* 2013). It is a cohesive soil with the smectite clay group minerals constituting the primary portion of the clay composition. It was supplied by Sibelco Australia Limited and contained finely powdered eggshell shade of white as illustrated in Fig. 3(a).

Ground Granulated Blast Furnace Slag (GGBFS) was procured from the commercial supplier BGC Cement Australia Pty Limited, whereas Capital Recycling Australia supplied the construction and demolition waste. GGBFS contains fine particles with a glassy crystalline texture and cementitious nature that enables it to show hydration upon addition of water. The texture and appearance of the two additives, GGBFS and CW have been respectively illustrated in Figs. 3(b) and 3(c). The chemical composition of GGBFS, as provided by the supplier has been reproduced in Table 2.

Procured construction waste primarily consisted of crushed masonry, tiles and concrete; which produced a widely varied texture, appearance, colour and composition of the CW. It was screened to remove glass and wood impurities and was dried in the oven at the temperature of $105 \pm 2^{o}C$ for a 24 hours period. It was then sieved and particles that fall in the range of particle sizes smaller than 4.75 mm sieve and larger than 2.36 mm sieve were separated. GGBFS hydration is a primarily time-dependent process and may behave differently under different curing periods depending upon its proportion in the bentonite-stabiliser system. Construction waste grains have a comparatively different size than bentonite and GGBFS and may change the gradation of the mixture in increasing number of volumes. Therefore, both parameters of stabiliser percentages and curing time were investigated.

Details of the specimens, grouped based on the composition, have been tabulated in Table 3.

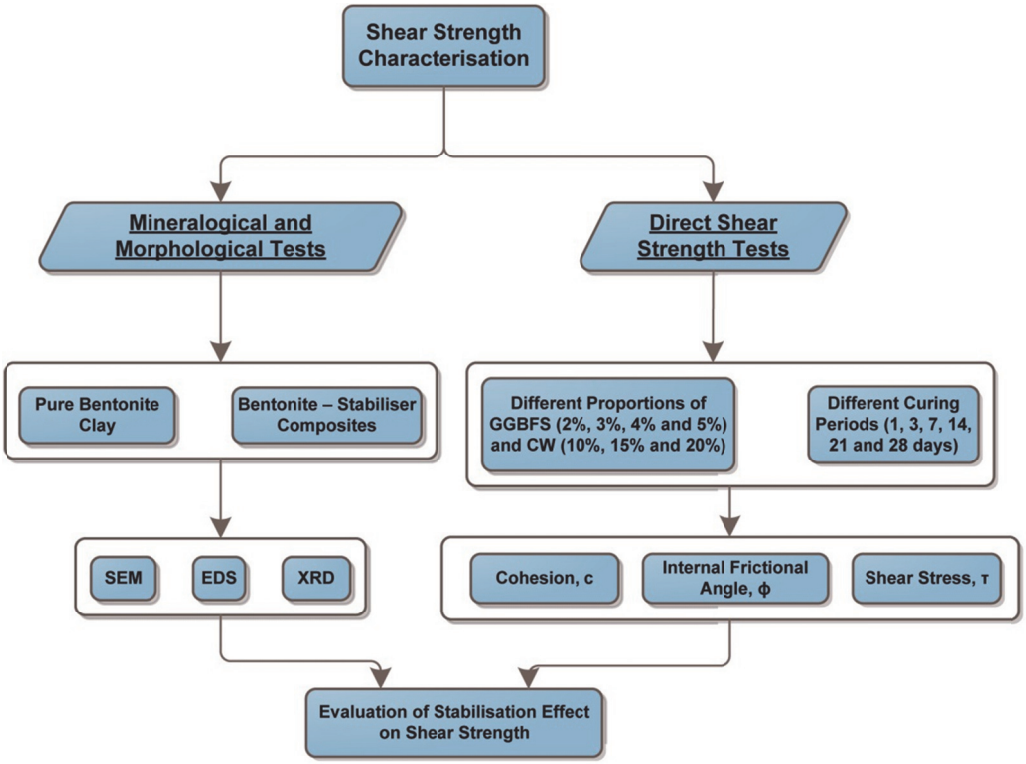

Fig. 2 Outline of the test design

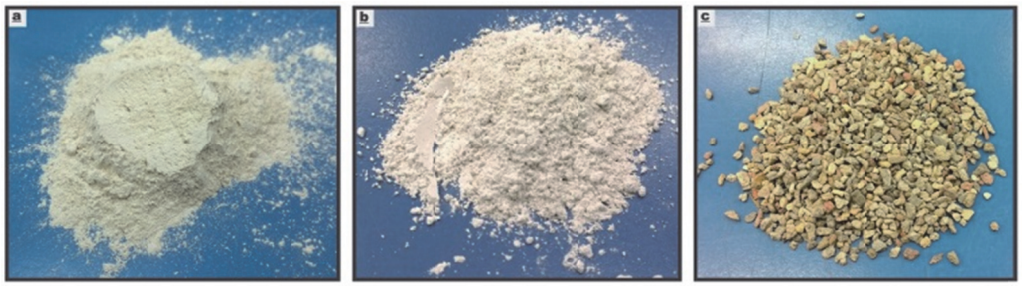

(a) Bentonite clay (b) GGBFS (c) Construction waste

Fig. 3 Test material images

Table 2 Chemical composition of GGBFS (BGC Australia)

Compound	Content
Calcium Oxide; CaO	30 ~ 50%
Amorphous Silica; SiO_2	35 ~ 40%
Aluminium Oxide; Al_2O_3	5 ~ 15%
Sulphur; S	< 5%

Table 3 Soil-stabiliser composite proportion scheme

Composition of samples	Group designation					Sample ID
Curing periods (days)	1	3	7	14	21	28
100% Bentonite	Group 1					S1G1
2% Slag + 10% CW + 88% Bentonite	Group 2					S1G2
2% Slag + 15% CW + 83% Bentonite						S2G2
2% Slag + 20% CW + 78% Bentonite						S3G2
3% Slag + 10% CW + 87% Bentonite	Group 3					G3S1
3% Slag + 15% CW + 82% Bentonite						S2G3
3% Slag + 20% CW + 77% Bentonite						S3G3
4% Slag + 10% CW + 86% Bentonite	Group 4					S1G4
4% Slag + 15% CW + 81% Bentonite						S2G4
4% Slag + 20% CW + 76% Bentonite						S3G4
5% Slag + 10% CW + 85% Bentonite	Group 5					S1G5
5% Slag + 15% CW + 80% Bentonite						S2G5
5% Slag + 20% CW + 75% Bentonite						S3G5

2.3 Laboratory Tests

Extensive distinct specimens were prepared with different ratios of construction waste and GGBFS and were tested under different curing conditions for shear strength evaluation succeeded by conduction of morphological and mineralogical characterisation through *x*-ray diffraction (XRD), scanning electron microscopy (SEM) and energy dispersive spectroscopy (EDS) techniques to study the effect on a microscale.

Shear Strength

Shear strength of bentonite-stabiliser composites were investigated using direct shear technique as specified by Standards Australia AS 1289.6.2.2 (1998). Hasan *et al*. (2016) performed standard compaction test on bentonite clay in accordance with the Standards Australia (2003) by subjecting clay samples to 596 kJ/m^3 compaction effort. Direct shear tests were conducted using Geocomp ShearTrac-II automated direct shear device, pictured in Fig 4(e). The device uses a horizontal and a vertical displacement transducer to assist in control of the horizontal and vertical loading system. Dedicated software is provided in the computer interface attached to the sensors and controls the micro-stepper motoring system for maintaining control of the constant displacement rate.

In order to maintain consistency of the mixture containing same proportion of construction waste and slag, both additives were mixed with bentonite in a large tray and water was carefully introduced under controlled proportions. The mixture was thoroughly mixed using manual mixing technique to produce and uniform granular texture, as illustrated in Fig. 4(a). After assembling the shear box illustrated in Figs. 4(b) and 4(c), samples were placed inside the shear box and saturated with water (Fig. 4(f)). The shear box employed for the study has an internal size of 63.5 mm × 63.5 mm × 24 mm. Normal stress was then applied on each sample to consolidate the samples. Five groups of samples, each with different additive percentages as specified in Table 3 were cured for 1, 3, 7, 14, 21 and 28 days of curing period, saturated and consolidated under the normal stress. Three levels of normal stresses; *i.e.* 50 kPa, 100 kPa and 200 kPa; and very slow horizontal strain rate (to control pore water pressure generation) were applied for testing each composition and curing day combination. The failure of sample was marked by shearing or splitting of the sample along the shearing plane, as highlighted in Figs. 4(d) and 4(g). Initially, the shear strength of pure bentonite was explored under increasing curing periods to obtain the benchmark results to assess the effect of both controlling parameters. The shear strength of soil was evaluated in relationship of the shear strength parameters (τ_f), soil cohesion (c), angle of internal friction (ϕ) and normal stress (σ).

$$\tau_f = c + \sigma \tan \phi \quad (1)$$

Microanalysis

The effect of stabilisers on bentonite particles at the microscopic scale was studied through microanalysis by developing *X*-ray diffraction (XRD) and scanning electron microscope (SEM) images. Variations in the physical appearance and elemental distribution of the mixture after the stabilisation process were then identified. Zeiss Evo 40XVP SEM analysis equipment was employed for the analysis of the particle arrangement, morphological composition and elemental distribution. The device is assisted by Oxford *x*-ray system that is controlled through INCA data acquisition and analysis software on the attached computer and is also capable of conducting energy dispersive spectrometer (EDS) analysis. The device utilises an electron beam for collection of micrographs. It was operated at beam current of 100 μA and 20 kV as acceleration voltage at working distance of 8.5 mm with 450 nm as the spot size. Further reliable data on the elemental composition and the mineralogy of the stabilised and unstabilised samples was collected through XRD quantitative analysis. The device used was Bruker-AXS D8 Advance Powder Diffractometer that utilised a Cu-Kα radiation beam operating at a current of 40 mA and voltage of 40 kV with a wavelength of 0.15404 nm collecting 2-theta data in the area of 7.5° ~ 90° scanning at the rate of 0.02°/seconds.

3. RESULTS AND DISCUSSION

The SEM micrographs and EDS analytical elemental or chemical characterisation on the samples generated comparatively precise information on the elemental composition of each of the specimens.

3.1 Material Microstructural and EDS Characterisation

Bentonite Clay

Bentonite is a reactive clay with montmorillonite as the central mineral and traces of accessorial minerals such as calcites, different classes of feldspar, iron oxides, quartz and other clay minerals (Karnland 2010). The physical and chemical characteristics of bentonite clay play a significant role in its mechanical behaviour and have been summarised in Table 4.

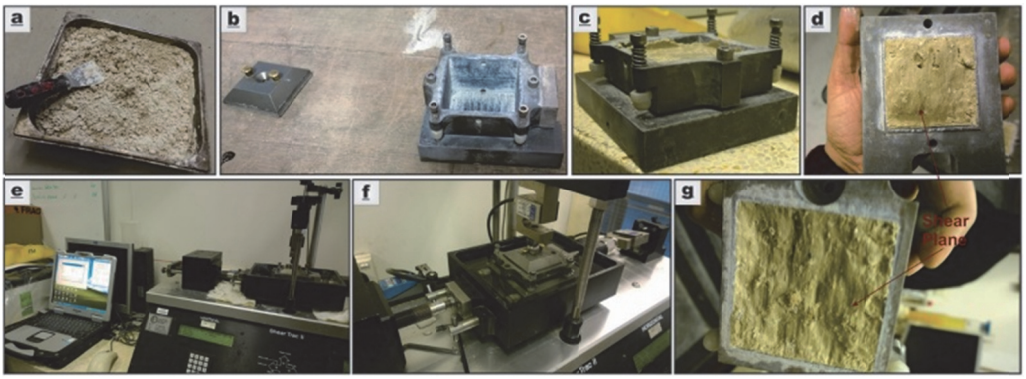

Fig. 4 Direct shear testing (a) prepared stabilised mixture, (b) shear box, (c) compacted specimen, (d) failed specimen, (e) DST device, (f) water-submerged specimen, and (g) failed specimen

It primarily contains sodium or calcium as the natural exchange cation with a higher absorptive capacity. It has a chemical formula of $Al_2O_3\,4SiO_2H_2O$ and chemically named as hydrated aluminium silicate. SEM and EDS microstructural and mineralogical characterisation analyses were performed to yield further data regarding the material composition and structure of pure bentonite clay. Figure 5 presents the micromorphology of bentonite clay.

Table 4 Properties of bentonite clay

Properties	Value
Chemical name	Hydrated aluminium silicate
Molecular formula	$Al_2O_3 \cdot 4SiO_2H_2O$
Physical appearance	Eggshell white granules
Specific gravity	2.65
pH	7 ~ 9
Odour	None
Flammability	Inflammable
Density	593 kg/m^3
Surface Area	0.09 ~ 1.8 m^2/cc

The micrographs of pure bentonite particles have been produced in Fig. 5(a). In general, it was observed that the bentonite particle sizes approximately ranged between 10 ~ 30 μm. The particle crystallography appeared to be amorphous with significant deviations in the particle shapes and sizes. Figure 5(b) illustrates the EDS spectra of the bentonite particles and quantitative analysis results are outlined in Table 5.

Table 5 Quantitative chemical composition of bentonite clay

Element	Weight %	Atomic %	k Ratio	Standard
O	55.91	70.25	0.34248	SiO_2
Na	1.12	0.98	0.00604	Na_2O
Mg	1.93	1.60	0.01458	MgO
Al	7.65	5.70	0.0664	Al_2O_3
Si	22.26	15.94	0.23039	SiO_2
S	0.78	0.49	0.0089	FeS_2
Ca	9.19	4.61	0.11461	CaO
Ti	0.32	0.13	0.00367	TiO_2
Fe	0.84	0.30	0.00936	Fe_2O_3
Totals	100.00	100.00		

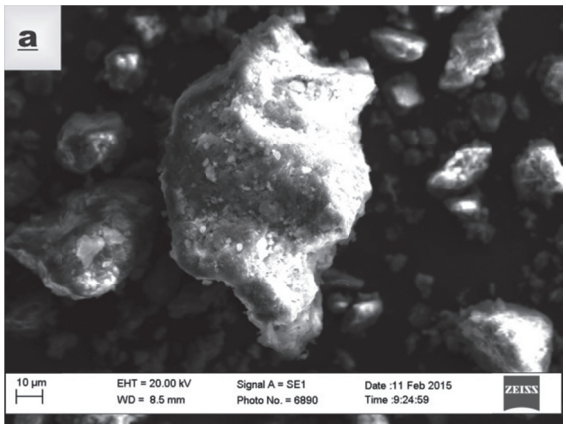

(a) SEM micrograph

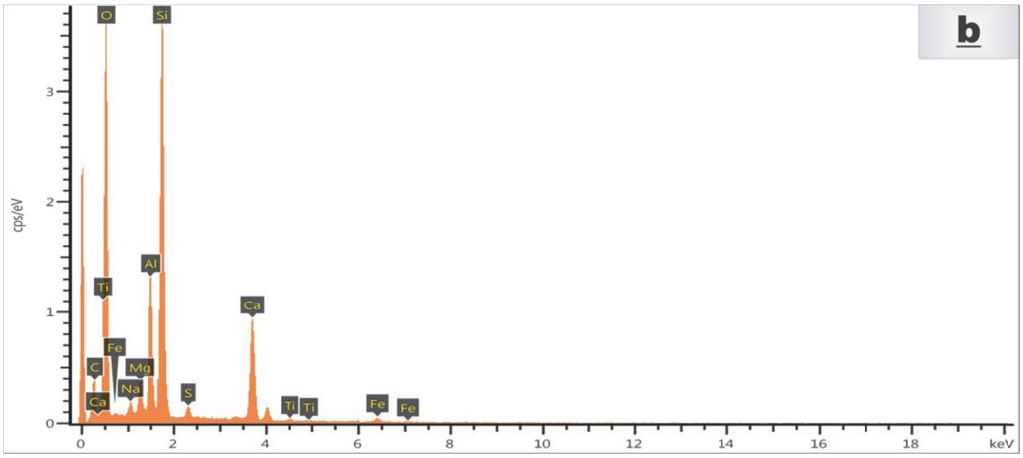

(b) EDS spectra

Fig. 5 Micromorphology of bentonite clay

The most dominant peak in the line spectrum is for silicon, followed by oxygen, iron and titanium. Quantitative analysis showed that silica and metallic oxides were normally found in the sample as the other dominant elements were calcium, aluminium, magnesium, sodium, sulphur and iron followed by titanium. This results support the elemental distribution of montmorillonite-smectites (Hasan *et al*. 2016; Deer *et al*. 2013).

GGBFS

The nature of the contributing materials; *i.e.*; fluxes, carbon and the originating iron ore dictate the chemistry and chemical composition of the resulting GGBFS. It is primarily composed of metallic oxides such as iron oxides (Fe_2O_3), manganese oxide (MnO), magnesium oxide (MgO), aluminium oxide (Al_2O_3), calcium oxide (CaO), and silica (SiO_2) and sulphur (S) (Proctor *et al*. 2000; Nidzam and Kinuthia 2010). Figure 6 illustrates the SEM micrographs of the GGBFS used in this study at scales of 20 μm and 1 μm.

Figure 6(a) shows that the GGBFS particles appeared to possess particle morphology that is dissimilar from bentonite particles as the particle sizes and shapes exhibited wide variations and random size distribution can be postulated for slag particles even though the appearance of the slag granules appeared to nominal variance in terms of particle texture. Moreover, the slag crystals generally displayed a glassy crystalline structure. As highlighted in Fig. 6(b), slag granules generally demonstrating straight-edged rougher texture with the grains sized at 11 μm ~ 40 μm.

The elemental distribution of the GGBFS employed in this study was also explored through EDS testing; the results of quantitative analysis and EDS spectra have been outlined in Table 6 and Fig. 7, respectively. Oxygen was observed as the most dominant element which was followed by calcium and sulphur. Silicon and metals like aluminium and magnesium succeeded as the most common elements which confirms the presence of silica and metallic oxides in GGBFS as has been found by other researchers (Gardner *et al*. 2015; Murthy *et al*. 2014; Fredericci *et al*. 2000), whereas the presence of sulphur can be attributed to the supplier signature as the exact chemical composition might vary between different commercial suppliers.

Construction Waste

The construction and demolition waste (CW) employed in this study was collected from a commercial recycling organisation and had originated from variety of construction projects including rubble, crushed masonry and concrete from residential and infrastructural projects. The texture, appearance and colour of CW grains largely varied due to the variation in the source and might have also caused variation in the elemental distribution of the CW particles.

Figure 8 illustrates the micrograph and EDS spectra of construction waste particles. Figure 8(a) illustrates that the CW grains exhibited rough texture with surface crack and voids or vesicles showing a lenticular appearance. It can be speculated that the formation of surface cracks and voids, due to bearing similarity with aggregates and gravels, may aid in generation of a higher angle of internal friction of the composite particles as the particles might interlock upon compaction. The results of quantitative analysis on construction waste grains have been tabulated in Table 7. Figure 8(b) and Table 7 display that silica, metallic and alkali oxides were found to be the most common compounds as is common with the plagioclase feldspars (Hasan *et al*. 2016; Deer *et al*. 2013).

3.2 Shear Strength

In this study, specimens prepared from bentonite and bentonite-stabilisers were subjected to normal stresses of 50 kPa, 100 kPa and 200 kPa after different curing periods and changes in the shear strength parameters including the shear stress (τ), internal frictional angle and cohesion. For the purpose of this study, DST was performed by using a shear box that shears the sample under a specified shearing rate (Fig. 9).

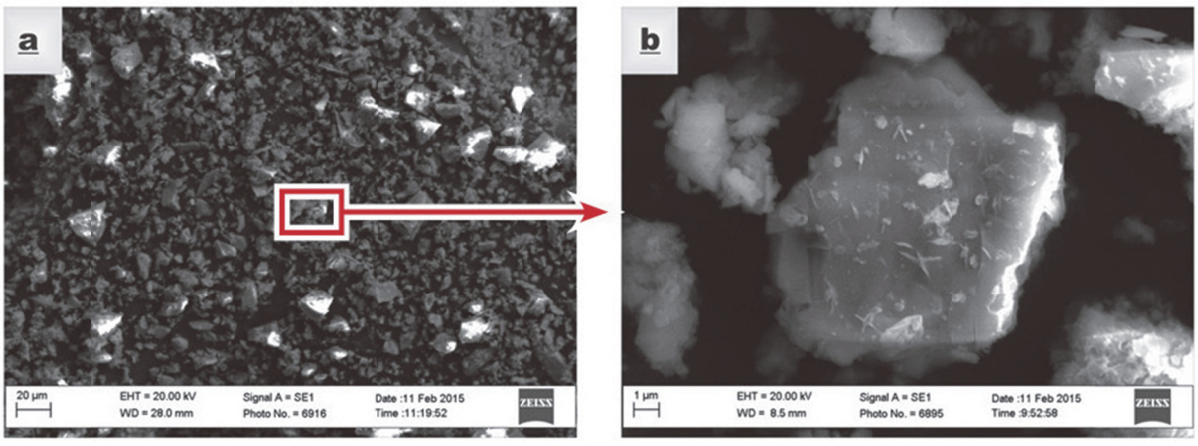

(a) 20 μm scale (b) 1 μm scale

Fig. 6 GGBFS SEM micrograph at (a) 20 μm scale, and (b) 1 μm scale

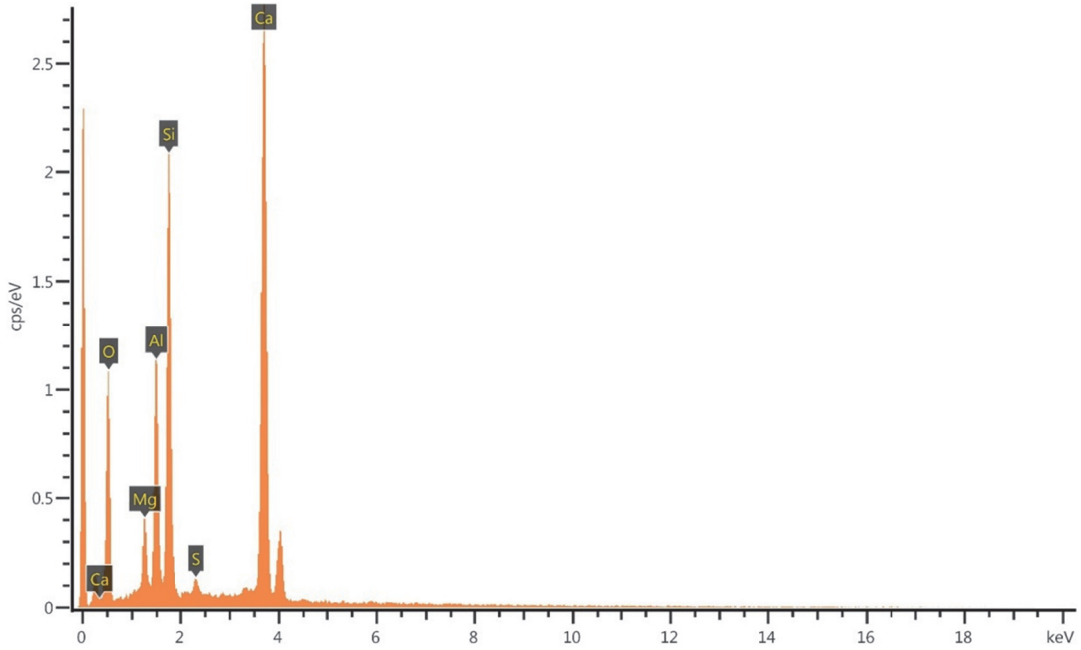

Fig. 7 GGBFS EDS spectra

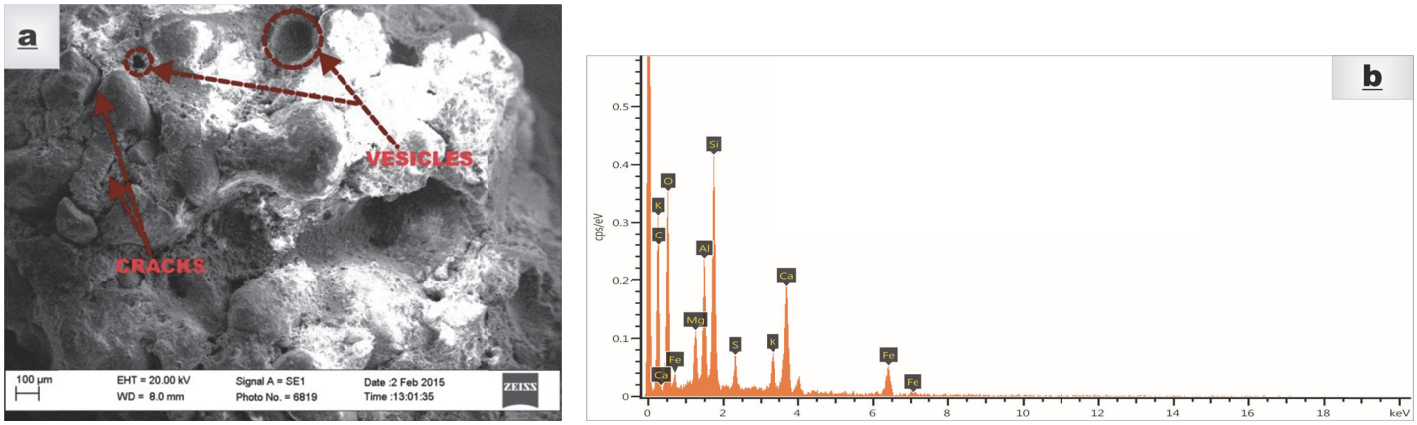

(a) SEM micrograph

(b) EDS spectra

Fig. 8 Construction waste

Table 6 Quantitative chemical composition of GGBFS

Element	Weight %	Atomic %	k Ratio	Standard
O	42.26	42.26	0.11971	SiO_2
Mg	2.87	2.87	0.02003	MgO
Al	7.88	7.88	0.06275	Al_2O_3
Si	14.54	14.54	0.13985	SiO_2
S	0.58	0.58	0.0066	FeS_2
Ca	31.88	31.88	0.38329	CaO
Total	100.00	100.00		

Table 7 Quantitative chemical composition of construction waste

Element	Weight %	Atomic %	k Ratio	Standard
O	45.12	62.76	0.17139	SiO_2
Mg	4.37	4.00	0.0249	MgO
Al	8.82	7.27	0.05653	Al_2O_3
Si	15.74	12.47	0.12137	SiO_2
S	2.52	1.75	0.02298	FeS_2
K	3.58	2.04	0.03518	K_2O
Ca	11.43	6.35	0.11292	CaO
Fe	8.43	3.36	0.07549	Fe_2O_3
Totals	100	100.00		

Figure 9(a) illustrates one of the bentonite-stabiliser samples, placed and compacted inside the metal box. Once lateral load was applied a sample shear failure would occur along the horizontal plane "XX", causing the specimen to split along that plane, as exhibited by Fig. 9(b). In order to quantify the effects of increasing curing periods or stabiliser proportions in the bentonite-stabiliser composites, a non-dimensional parameter based upon the strength development index introduced by Hasan *et al*. (2016) was adapted. The shear stress index "τ_I" employed in this study is empirically defined as:

$$\tau_I = \frac{\text{Shear stress of pure bentonite sample}}{\text{Shear stress of bentonite - stabiliser composite sample}} \leq 1 \quad (2)$$

The value of shear stress index indicates the efficiency of the stabilisation process and is directly correlated with the peak shear stress sustained by the specimen before failure. Higher τ_I values are attributed to lower shear strength of the stabilised composite and on the other hand, lower τ_I values are indicative of an enhancement effect in the shear strength. The upper limit of "1" indicates that the addition of stabilisers cannot generate reduction in the shear strength. The shear stress index has been extensively used in this research for identifying the effect of stabilisers which became more significant as the curing of the samples was continued. Shear strength of bentonite clay appeared to be largely unaffected by curing period, provided the normal stress has been kept constant as the increase in the induced vertical stress triggered an increase in the shear strength (Fig. 10). Generally, results of pure bentonite clay samples exhibited same cohesion and similar internal frictional angle values.

The effects of curing time become more pronounced with the addition of stabilisers. For all bentonite-stabiliser composites, the shear strength generally increased with curing period irrespective of the normal stress applied to the specimens. Optimum increase in shear strength was observed for the sample S3G5, which displayed a τ_I value of 0.71 corresponding to a shear stress of 193.05 kPa at 0.51 mm for the bentonite-stabiliser composite and shear stress of 137.10 kPa at 0.91 mm for the pure bentonite clay specimen, when subjected to normal stress of 200 kPa and a curing period of 28 days as illustrated by shear values displayed in Fig. 11. This also shows that for the specimens S3G5 subjected to 200 kPa of normal stress, 28 days of curing produced an increase of 17.58 kPa in the shear stress compared to the 175.47 kPa of S3G5 specimen after 1 day of curing to a corresponding horizontal displacement of 0.61 mm (Fig. 11). Therefore, slight reduction in the horizontal displacement observed upon peak shear stress was also observed.

The development of shear strength was observed for all stabiliser-bentonite composite specimens; however, the strength development was gradual and indicated that the curing of specimens produced increase in the shear strength under all normal stress conditions. On the individual parametric scale, sample cohesion tended to exhibit a uniform trend of increasing values with escalating curing period regardless of the stabiliser dosage in the composite. The trend was steeper during the initial period of curing and normally tended to gradually rise after 7 days of curing, whereas the highest cohesion values were observed at 28 days curing period as shown in Fig. 12. The cohesion value of pure bentonite sample ranged from 55.60 kPa for 1 day curing to 58.90 kPa after the sample had been cured for 28 days. Similar to the trend observed for shear stress values, the cohesion values

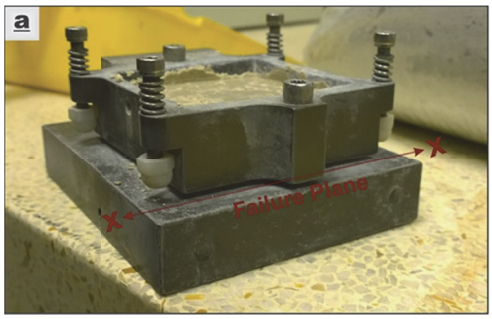

(a) Compacted specimen in shear box

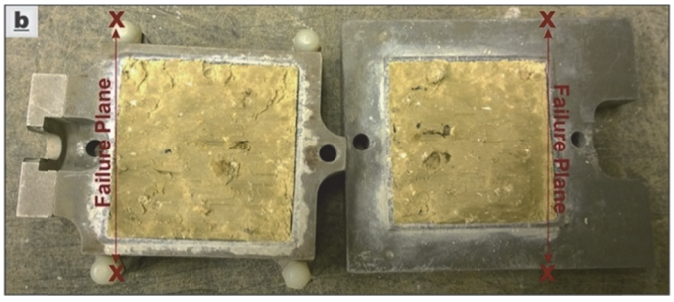

(b) Sheared/failed specimen

Fig. 9 Direct shear sample assembly

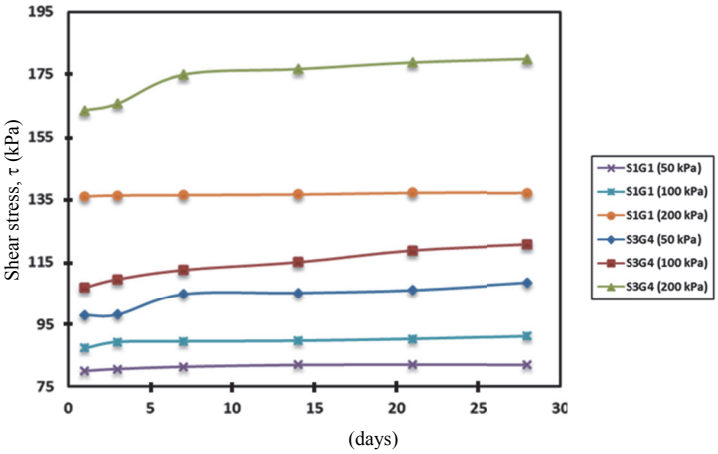

Fig. 10 Shear stress-curing time relationships for pure bentonite (S1G1); and 76% bentonite, 4% GGBFS and 20% CW (S3G4) bentonite-stabiliser composite for 50 kPa, 100 kPa and 200 kPa normal stresses

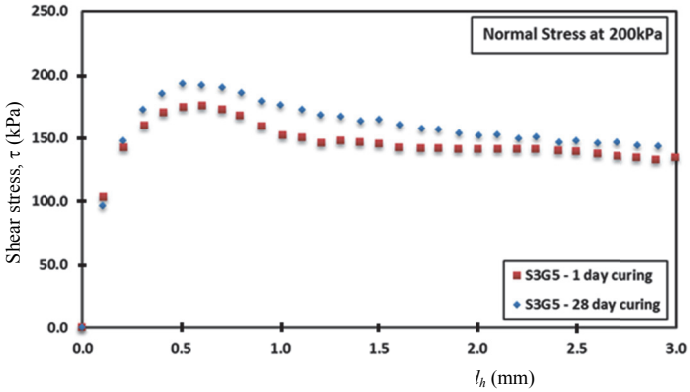

Fig. 11 Shear stress-horizontal displacement curves for S3G5 at 200 kPa normal stress after 1 day and 28 days of curing

showed more development with the increasing proportion of the stabilisers as the cohesion value for sample S3G2 ranged from 56.84 kPa to 59.76 kPa for the curing periods of 1 day and 28 days, respectively. Sample falling under the S3G5 category exhibited the most prominent development in the cohesion value as 28 days of curing produced cohesion of 67.26 kPa compared to cohesion value of 61.9 kPa after the sample was cured for only one day.

Similar to the trends observed for cohesion, the internal frictional angle values increased with the increasing curing period. Even though the variations in the frictional angle with curing period inclined to be higher with further curing, the rise was gradual for majority of the samples and exhibited an arbitrary increase in succeeding frictional angle values for most of the test composite specimens as Fig. 13 shows. It can be observed that all bentonite-stabiliser composites exhibited increased angles of internal friction as the curing of specimens progressed. Pure bentonite clay specimens displayed an internal friction angle value of 20.15° ± 0.25°, a variation of approximately 1.2% between all the investigated curing periods. For bentonite-stabiliser composites, a direct correlation was observed between the gradual increase in ϕ values and sample curing periods. Curing period of 28 days generated the maximum internal friction angle for all sample groups. Although the results showed that the growth in the value of internal friction angle became more pronounced as the proportion of the stabilisers increased in the bentonite-stabiliser composite, interestingly, as the proportion of slag was lower in the bentonite-stabiliser composites, increasing percentage of construction waste produced a lower frictional angle value.

Approximately all of the bentonite-stabiliser composite samples had gained maximum degree of internal friction angle by 21 days of curing and further curing only produced nominal increase in the frictional angle value, with the value remaining within the range of 0.001° ~ 0.836°. The maximum increase in the internal friction angle due to curing was observed for specimens in the S3G5 category where the internal friction angle showed an increase of 2.3° after curing of 28 days attributed to a post-28 days' internal frictional angle value of 27.3° compared to the frictional angle value of 25.0° after 1 day of curing. The results showed a regular correlation between the proportions of the stabilisers in the bentonite-stabiliser composites and the development of frictional angle similar to sample shear stresses and cohesion values. Evaluation of the calculated shear strength parameters showed that the introduction of stabilisers produced significant improvements in the shear strength and the effect of each additive was also evaluated. Figure 14 shows the relationship between the percentage of GGBFS in the bentonite-stabiliser composite specimens, prepared with different percentages of construction waste (10%, 15% and 20%), and the internal angle of friction (ϕ). Moreover, the effect of increasing the percentage of construction waste in the bentonite-stabiliser composite for a specific proportion of GGBFS has been illustrated in Fig. 15.

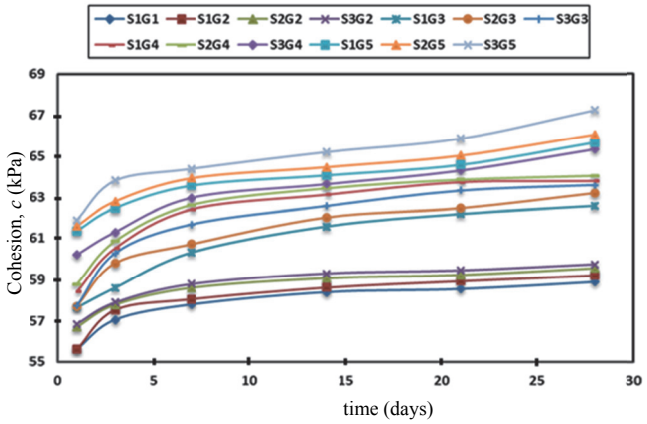

Fig. 12 Cohesion-curing time relationships for pure bentonite and all tested bentonite-stabiliser composite specimens

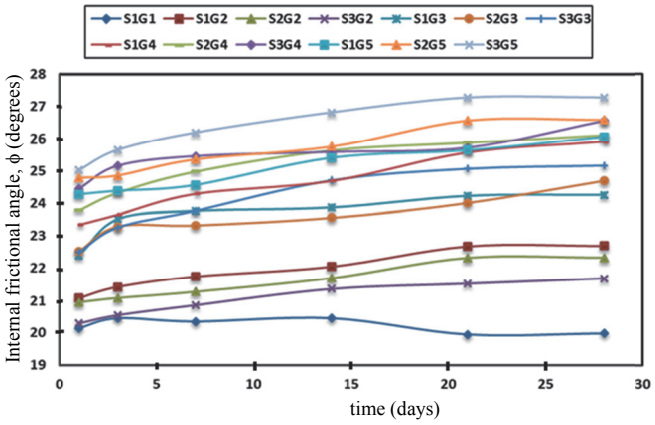

Fig. 13 Internal frictional angle-curing time relationships for pure bentonite and all tested bentonite-stabiliser composite specimens

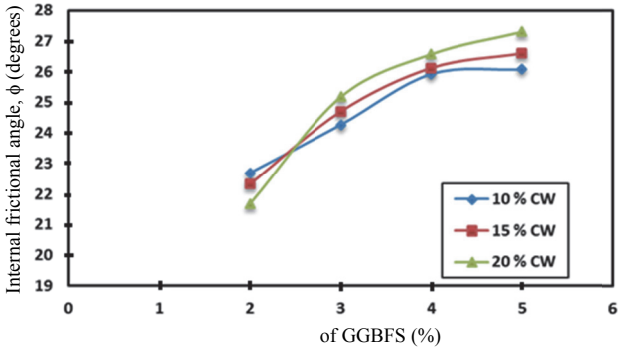

Fig. 14 Development of internal frictional angle with percentage of GGBFS for 28 days curing period

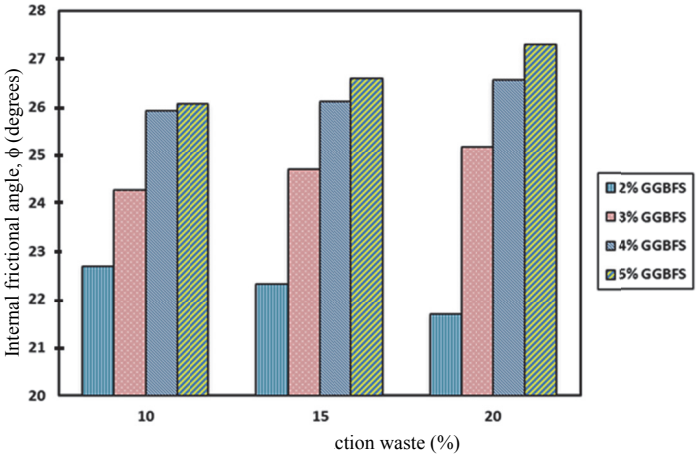

Fig. 15 Development of internal frictional angle with percentage of CW for 28 days curing period

Introduction of smaller amount of GGBFS at 2% caused the internal friction to increase by 2.7° when the percentage of construction waste was kept at 10% to generate a value of 22.7°, but the progression of frictional angle became more prominent after the percentage of slag was further increased as for 3% proportion of GGBFS in the bentonite-stabiliser composite also containing 10% CW, the frictional angle further developed to be 24.3° showing increase of 4.3° in the S1G3 category samples compared to pure bentonite samples at 28 days curing period. Moreover, addition of construction waste reduced the internal friction angle when the proportion of slag was lower in the composite mixture. For sample group 2, the frictional angle value dropped by 0.4° and further plummeted by 0.6° attributed to frictional angle values of 22.3° and 21.7° for the respective CW proportion of 15% and 20% in the mixture after 28 days of specimen curing. However, the decrement in frictional angle by increasing construction waste percentage was limited to lower proportion of slag as for sample group 3 which contained 3% of GGBFS, the frictional angle value developed by 0.43° to 24.7° as the CW percentage was increased from 10% to 15% and then 25.2° as amount of CW was set at 20%, for 28 days of curing period. Similar trends were observed for samples containing 4% and 5% GGBFS cured for 28 days with the enhancement effect of GGBFS more prominent as the curing progressed. In general, variations in internal friction angle for 3% GGBFS sample group remained < 4% due to changes in CW quantities, whereas increments in percentage of slag to 4% caused a rise of more than 6%. Furthermore, the ϕ value developed to 26.1° when the slag content was increased to 5% for constant percentage of CW at 10%. The optimum GGBFS dosage for increasing the ϕ value was found to be 5% which produced an increase of approximately 6° with sample S1G5 displaying a ϕ value of 26.1° after 28 days of curing and 10% CW, however, introduction of further construction waste caused the angle to increase up to 27.3° as the CW percentage increased to 20%.

Similarly, the cohesion values of test specimens exhibited the tendency to increase as the stabiliser percentages were increased, as exhibited in Figs. 16 and 17. This trend continued in sample groups regardless of the type of stabiliser that was increased in the composite. As the cohesion values remained affected by the sample curing time, the increment in the cohesion value was similar for all samples with the same proportion of both additives in the bentonite-stabiliser composite. Cohesion value obtained for pure bentonite clay was 58.90 kPa which was only nominally enhanced by 0.5% to give a cohesion value of 59.21 kPa when 2% of GGBFS and 10% CW were added to bentonite in the sample mixture. Nonetheless, further increment was observed as the cohesion value increased to 59.57 kPa when the percentage of CW was increased to 15% while the GGBFS proportion remained unchanged and increased to 59.76 kPa as the amount of CW in the mixture grew to be 20%. Similar trend was observed upon further increment of the additives as the cohesion value increased to 62.60 kPa for 3% of GGBFS and 10% CW and 64.06 kPa for the CW content of 15% and GGBFS percentage of 4% in the bentonite-stabiliser composites. The highest development in the cohesion value was observed for the sample S3G5 with around 14.2% increase compared to the pure bentonite sample as the cohesion value increased to be 67.26 kPa when the volumes of GGBFS and CW were 5% and 20% respectively.

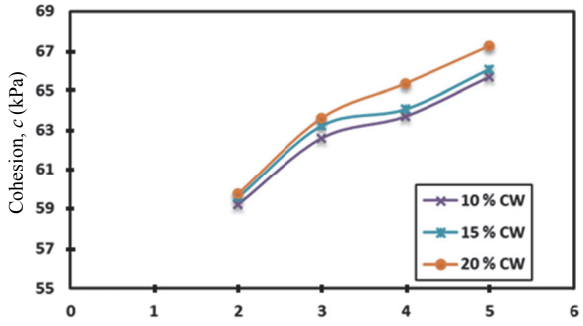

Fig. 16 Development of cohesion with percentage of GGBFS for 28 days curing period

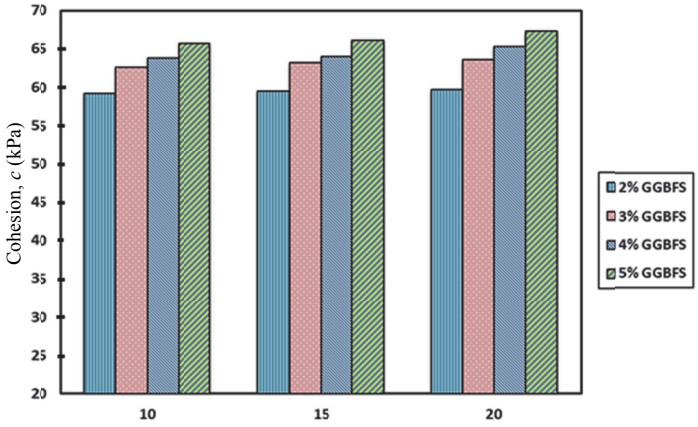

Fig. 17 Development of cohesion with percentage of CW for 28 days curing period

This observation can be attributed to the variations in the physical characteristics such gradation and hydraulic nature of the bentonite-stabiliser composites triggered by the increasing proportion of the two additives in the sample mixture.

Some of the typical shear stress-horizontal displacement curves for pure bentonite clay and bentonite-stabilisers composites after 28 days of curing have been illustrated in Figs. 18 ~ 20. These sample groups have been selected to represent the general trend that was observed for the entire specimen matrix, and therefore, the graphs were drawn based upon the minimum, moderate and maximum additive percentages. The initial slopes of the $\tau \sim d_h$ curves for all samples exhibited similarities provided the normal stress had been kept constant. At a normal stress of 50 kPa, pure bentonite clay sample showed a peak shear stress value of 81.90 kPa occurring at displacement of 0.50 mm and was improved upon introduction of 3% GGBFS and 10% CW to 97.06 kPa, corresponding to a τ_I value of 0.84. The τ_I further reduced to 0.82 as the percentage of CW increased to 15%, resulting in failure at shear stress of 99.35 kPa and 0.70 mm displacement, and at shear stress of 101.68 kPa when the CW proportion became 20% for the constant GGBFS proportion of 3%, as demonstrated in Fig. 18. It also shows that as the percentage of GGBFS was raised to 5%, the peak shear stress exhibited by the sample prior to failure reached 109.44 kPa occurring with horizontal displacement of 0.50 mm. The specimens with 5% GGBFS and vertical stress of 50 kPa showed a similar trend of increasing peak shear stress value upon increments of the CW

content in the mixture as the samples from group 3 that contained 3% of GGBFS as the peak shear stress upon failure which developed as the quantity of CW in sample escalated to 15%, corresponding to peak shear stress of 111.02 kPa and then 115.95 kPa for 20% CW.

Figure 19 displays that when the normal stress was increased to 100 kPa, pure bentonite clay sample S1G1 demonstrated failure when the horizontal displacement had reached 0.7 mm for a shear stress value of 91.10 kPa. After adding 3% GGBFS and CW percentage of 10%, the shear resistance of the sample was improved as it failed at peak shear stress of 108.76 kPa, this corresponds to failure at a horizontal displacement that is 0.3 mm less than the pure bentonite sample. Similar to the trend observed for samples subjected to 50 kPa of normal stress, peak shear stress value further increased to 110.64 kPa as the proportion of construction waste increased for sample S2G3 which contained 3% GGBFS and 15% CW corresponding to a failure strain of 0.80 mm. The tendency for shear stress increment in case of 100 kPa normal stress samples with addition of further amount of GGBFS was also similar to the samples exposed to a normal stress of 50 kPa. The peak shear stress increased to 121.88 kPa for a displacement of 0.81 mm for sample S1G5 which constituted of 5% GGBFS and 10% CW in the bentonite-stabiliser composite. Furthermore, the shear strain also exhibited a similar trend as the sample had failed a displacement value that is 0.3 mm higher than sample S1G3. In addition, the maximum shear stress was again associated with sample S3G5 that exhibited a peak shear stress value of 129.13 kPa and the pure bentonite clay sample yielded the lowest shear stress value of 91.10 kPa.

The shear stress-horizontal displacement relationships for the direct shear strength tests on pure bentonite and bentonite-stabiliser composite samples that were subjected to 200kPa of normal stress are illustrated in Fig. 20 which also displayed similar shear strength trends as the 50 kPa and 100 kPa samples. The shear stress shown by pure bentonite clay sample at failure was 55.2 kPa higher than that exhibited by the same sample at 50 kPa, corresponding to respective peak shear stresses of 137.1 kPa for strain value of 0.91 mm. Development in shear strength was observed for the bentonite-stabiliser composite sample compared with the pure bentonite clay sample as the inclusion of 3% slag and 10% construction waste yielded a shear stress value of 163.88 kPa whereas the strain value had approximately reached 0.80 mm, which was 0.11 mm lower than the pure bentonite clay sample. Moreover, the peak shear stress generated by sample containing additional 5% of construction waste, *i.e.*, sample S2G3, was approximately 1.74 kPa higher than sample S1G3, failing at 165.62 kPa at displacement of 0.51 mm. These results correspond to the observation from the earlier samples that indicated a correlation between evolution of shear stress in the samples and the increasing percentages of the stabilisers. This hypothesis was further supported by the increment of peak shear stress for sample S1G5 that had 10% construction waste with 5% slag exhibiting failure at maximum shear stress of 182.22 kPa, corresponding to τ_I of 0.75. The lowest value of τ_I at 0.71 was observed for sample S3G5, which shows the maximum improvement in the shear strength, as the sample displayed peak shear stress of 193.05 kPa showing an enhancement effect of 55.95 kPa for the bentonite-stabiliser composite as compared with the pure bentonite clay sample.

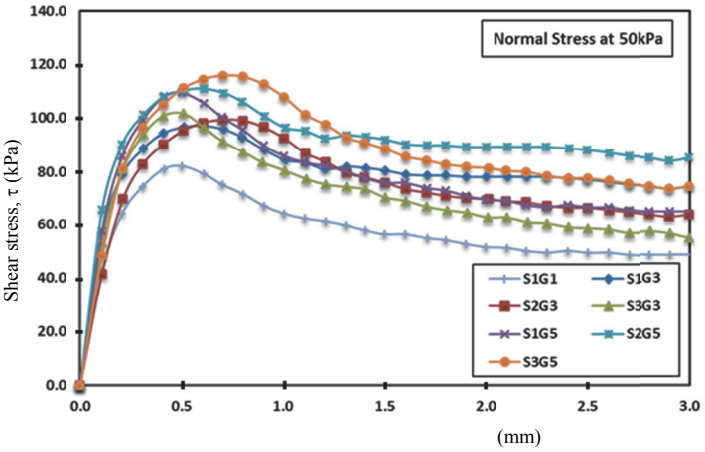

Fig. 18 Shear stress-horizontal displacement curves for samples S1G1, S1G3, S2G3, S3G3, S1G5, S2G5 and S3G5 at 50 kPa normal stress after 28 days of curing

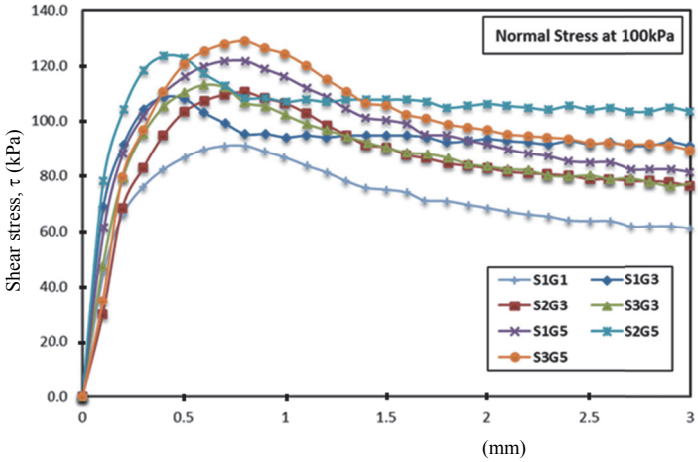

Fig. 19 Shear stress-horizontal displacement curves for samples S1G1, S1G3, S2G3, S3G3, S1G5, S2G5 and S3G5 at 100 kPa normal stress after 28 days of curing

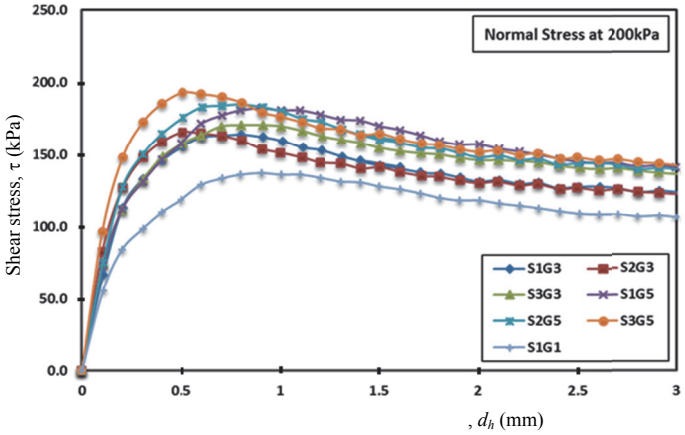

Fig. 20 Shear stress-horizontal displacement curves for samples S1G1, S1G3, S2G3, S3G3, S1G5, S2G5 and S3G5 at 200 kPa normal stress after 28 days of curing

The maximum shear stresses of pure bentonite and bentonite-stabiliser composite samples obtained after 28 days of curing are presented in Table 8. Comparative analysis of sample failures for pure bentonite sample and 2% slag and 10% construction waste content sample shows that even though the sample failure for the later occurred at a higher shear stress than the pure bentonite specimen, the difference in maximum shear stresses was not significant and ranged between 1.65 kPa ~ 3.97 kPa for different normal stresses. The gap between the peak shear stresses of pure bentonite and bentonite-stabiliser composite samples widened with the increment of the normal stress as the same sample S1G2 achieved a peak shear stress value of 95.22 kPa at 100 kPa whereas sample S1G1 failed at 91.10 kPa. Notable development of shear stress was observed when the slag content was doubled for sample S1G4 which contained 4% slag and 10% CW, as the maximum shear stress value before failure had reached 102.24 kPa for normal stress of 50 kPa. Moreover, the variation between the unstabilised and stabilised samples became more noticeable as the sample was subjected to a normal stress of 100 kPa when the sample S1G4 displayed a shear stress value of 114.24 kPa which was 23.14 kPa higher than the pure bentonite clay sample. Overall, the tested samples exhibited maximum improvement in the shear strength under normal stress of 200 kPa when the specimen curing time had reached 28 days. In general, direct correlation was observed between the net normal stress imposed upon the sample and the maximum shear stress exhibited by sample prior to failure. Moreover, the value of τ_I generally tended to reduce with increasing stabiliser percentages as illustrated in Fig. 21.

For the minimum stabiliser dosage, *i.e.*, 2% of GGBFS with CW proportion of 10%, the shear index value was observed as 0.97. This value continued to reduce as the additive proportions increased, as for sample S2G2, shear index dropped to 0.95 and further reduced to 0.83 for sample S1G3. Overall, sample group 2 showed the highest values of shear indices which ranged from 0.971 to 0.94. As the GGBFS content in the sample increased to 3%, the median values of shear indices were observed for the sample group 3, ranging from 0.83 for S1G3 on the higher side to the lowest value of 0.8 for S3G3. However, the lowest shear indices among all sample groups were observed for the sample group 5 with 5% GGBFS content with 0.71 as the lowest shear index value, overall.

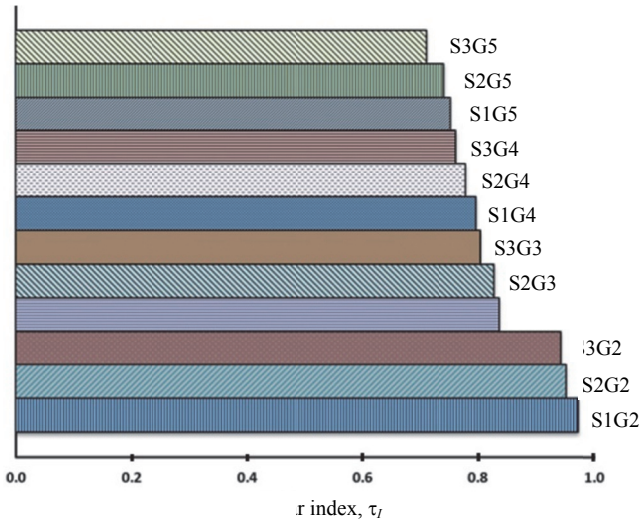

Fig. 21 Shear indices for test specimens under 200 kPa of normal stress and 28 days curing period

The development of shear stress with additives shows that both recycled aggregates and slag have positive effects on the shear strength behaviour of the bentonite clay tested in this research, for the studied curing and additive controlled conditions. Although the addition of construction waste had initially resulted in reduction of the cohesion value, as can be observed for adding gravely soil in clay, increase in the internal friction angle was noted followed by increase in cohesion after the passage of significant periods of sample curing time, which corresponded to higher shear value and lower τ_I value for specimens after 28 days of curing.

3.3 Microanalysis of Materials

The effects of stabilisation process on the microscopic scale were studied through SEM and EDS tests on bentonite-stabiliser composites after 28 days of curing period, as has been presented in micrographs illustrated in Fig. 22.

The results of SEM analysis on bentonite-stabiliser composites reveal that the cavities and cracks on the surface of construction waste grains as well as the inter-particle voids were filled in by slag and bentonite particles as highlighted in Fig. 22(b). This might have aided in the improving the interlocking mechanism between the particles and therefore developing the internal frictional angle.

The results of EDS spectra analysis further show the presence of bentonite and slag particles clung to construction waste grains. Oxygen and silicon were the most common elements in the bentonite-stabiliser specimen matrix. The peaks illustrated in Fig. 23(a) indicate that silicon and oxygen formed the major composition of the sample mineralogy. Other elements included aluminium, iron, magnesium, sodium, titanium and calcium while silica and oxides of the dominant metals were the most dominant compounds. Overall, the results exhibited consistency with the findings from SEM and EDS tests on pure bentonite clay. Fig. 23(b) spectra peaks analysis results display similar peaks of silica and metallic oxides and those observed for GGBFS, whereas the quantitate analysis results and spectra peaks from Fig. 24(c) resembled the mineralogy results of EDS analysis for the construction waste particles.

Table 8 Maximum shear stresses under different normal stresses after 28 days of curing

Normal Stress (kPa)	Shear Stress at Failure (kPa)												
	S1G1	S1G2	S2G2	S3G2	S1G3	S2G3	S3G3	S1G4	S2G4	S3G4	S1G5	S2G5	S3G5
50	81.9	83.6	85.3	86.1	97.1	99.3	101.7	102.2	104.3	108.1	109.4	111.0	115.9
100	91.1	93.6	95.2	96.1	108.8	110.6	113.2	114.2	115.8	120.4	121.9	123.6	129.1
200	137.1	141.1	144.1	145.5	163.9	165.6	170.5	172.1	176.1	179.9	182.2	184.9	193.1

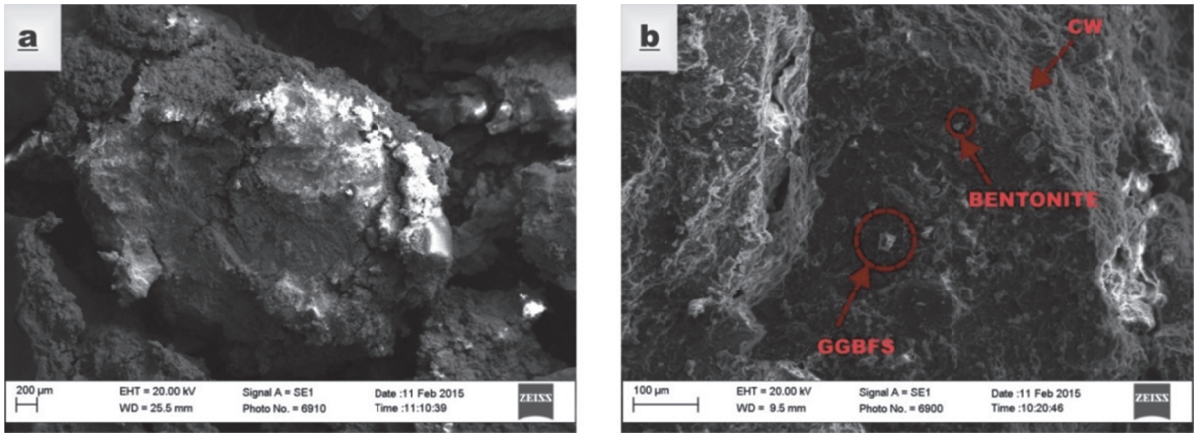

(a) 200 µm (b) 100 µm

Fig. 22 SEM micrograph of bentonite-stabiliser composite specimen after 28 days of curing at (a) 200 µm, and (b) 100 µm scales

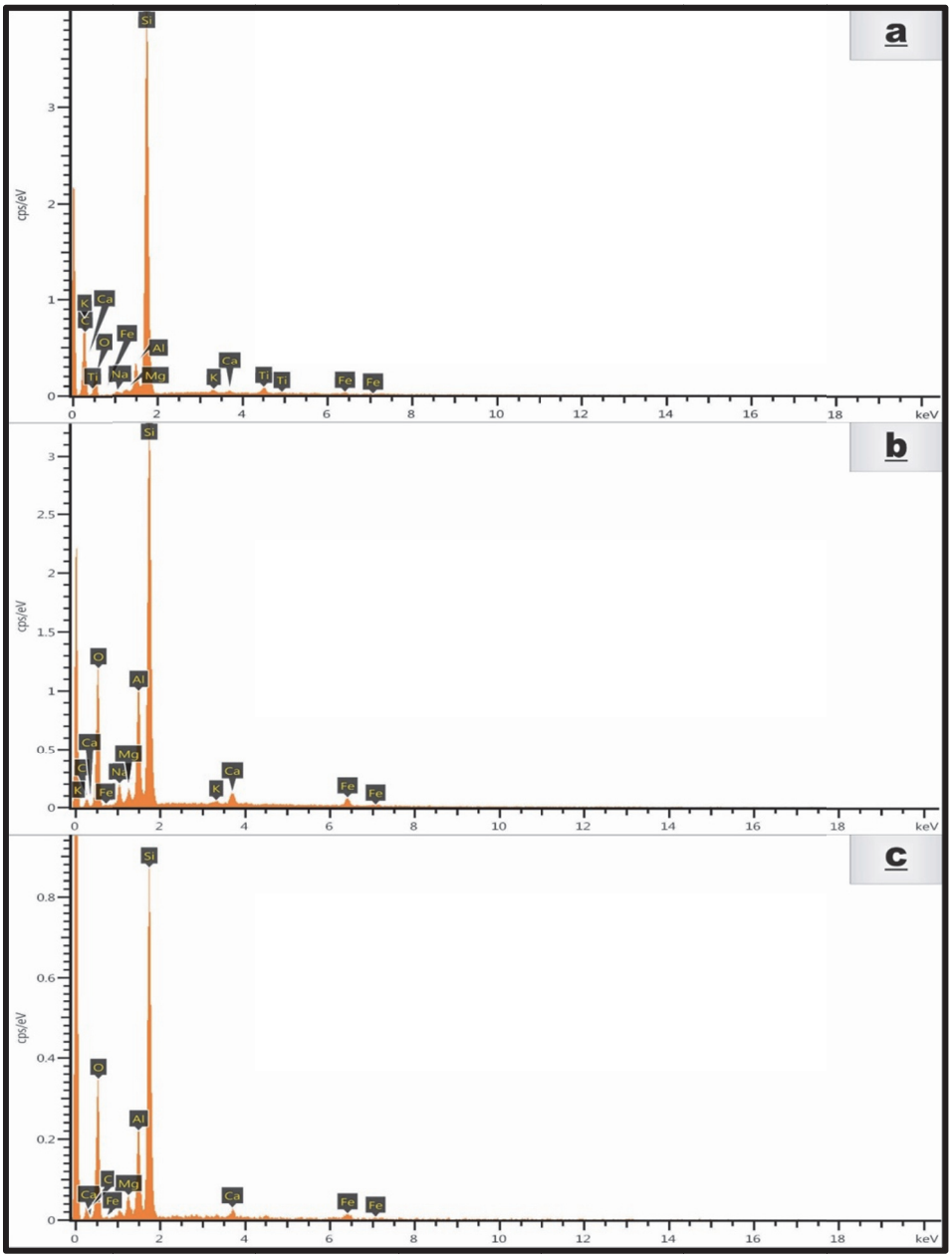

Fig. 23 EDS spectra of S3G5 after 28 days of curing with (a) bentonite, (b) GGBFS, and (c) construction waste grains

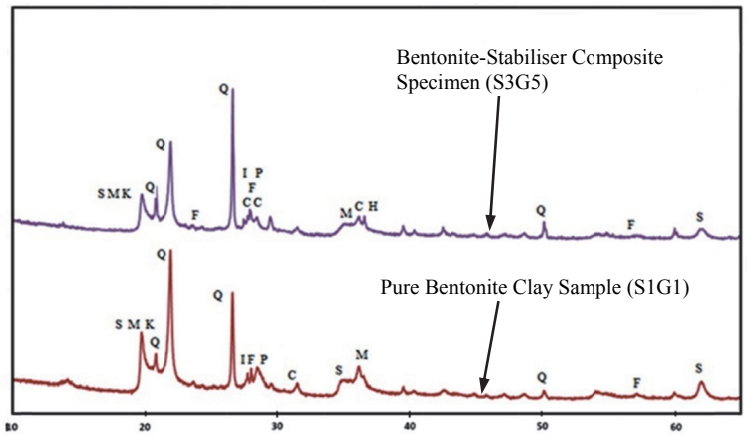

Fig. 24 X-ray diffraction spectrum of pure bentonite clay and bentonite-stabiliser composite specimens after 28 days of curing (S: smectite, M: mica, K: kaolinite, Q: quartz, F: feldspar, I: illite, CC: calcium carbonate, P: plagioclase, CH: calcium hydroxide, C: calcite)

Mineralogical XRD Analysis

The EDS spectra and SEM images indicated the presence of bentonite and GGBFS particles in the cavities and cracks found on the surface of construction waste grains. XRD tests were conducted to obtain insight into the mixture mineralogy and elemental distribution. The test results have been presented in Fig. 24 and provide the diffraction bands for the benchmark pure bentonite clay sample (S1G1) and bentonite-stabiliser composite specimen S3G5 that displayed the maximum improvement in shear strength under the imposed normal stresses and after 28 days of curing period.

Comparative analysis of both samples indicates the influence of clay stabilisation process using the two additives. Similar to the EDS results for both pure bentonite and bentonite-stabiliser composite specimens, quartz [SiO_2] was associated with the most dominant peaks for both stabilised and unstabilised samples, followed by other clay minerals like kaolinites [$Al_4[Si_4O_{10}](OH)_8$], illites [$K_{0.65}Al_2[Al_{0.65}Si_{3.35}O_{10}](OH_2)$], mica and alkali feldspars. Furthermore, the diffraction spectrum of bentonite-stabiliser composite specimen shows that in addition to the peaks observed for the pure bentonite clay sample, the stabilised sample exhibited peaks associated with calcium hydroxide [$Ca(OH)_2$]. This may be indicative of the hydration of stabilised mixture to yield $Ca(OH)_2$ from hydration of calcium oxide that was also found in the test material EDS spectra. These XRD characterisation results also correspond to the XRD test conducted on specimens of same composition and curing period conditions conducted by Hasan *et al*. (2016).

4. CONCLUSIONS

Many remedial methods exist for the treatment of such soils and the selection of any particular treatment method is largely dictated by its ability to enhance the strength of the soil. This study was conducted as an extension of the previous study performed for the feasibility investigation of bentonite clay stabilisation using GGBFS and construction waste under different proportions and curing conditions. The cured specimens were subjected to a series of direct shear tests under normal stresses of 50 kPa, 100 kPa and 200 kPa. The two stabilisers exhibited the potential of enhancing the shear strength parameters of bentonite clay. The following conclusions were drawn from this study:

1. Development in both internal frictional angle and cohesion was noted with additive introduction. After 28 days of curing, internal frictional angle of sample with 2% GGBFS and 10% CW reached 22.7°, escalating from initial value of 20.0°. However, ϕ value displayed a reduction to 22.3° when the proportion of CW increased to 20%. A reversal in this trend of declining ϕ value with increasing CW proportion was observed with increased GGBFS percentages in the mixture.
2. Conversely, addition of CW in the bentonite-stabiliser mixture tended to slightly vary the cohesion values as cohesion of 59.57 kPa was observed for sample with 2% GGBFS and 20% CW compared to cohesion of 59.21 kPa for sample with a 5% lower CW proportion is the sample.
3. Sample curing period and stabiliser addition also tended to increase the shear strength of specimens and this effect was studied through the introduction of a dimensionless unit, termed as shear index (τ_I). The peak shear stress values tended to rise with the rising percentages of the two additives. Under 50 kPa of normal stress and 1 day specimen curing, pure bentonite sample failed at 79.90 kPa, whereas with 20% CW and 5% GGBFS in the mixture, specimen failure was observed at 104.97 kPa, this shows a τ_I value of 0.76 after stabilisation. The distinction between peak shear stresses of stabilised and unstabilised specimens under constant normal stresses was more noticeable as the curing period escalated. After 28 days of curing, the sample with the least proportion of GGBFS and CW, respectively at 2% and 10%, and the sample with the maximum stabiliser proportions at 5% and 20%, respectively, showed respective peak shear stress values of 81.90 kPa and 115.95 kPa.
4. Furthermore, peak shear stresses were observed as functions of normal stresses, which in turns produced further gap between the shear strengths of stabilised and unstabilised mixtures. For the same samples, one with 2% GGBFS and 10% CW and the second with 5% GGBFS and 20% CW, at 100 kPa and 200 kPa of normal stresses, the differences between the observed peak shear stress values reached 38.03 kPa and 55.95 kPa, respectively.

5. The lowest τ_1 value of 0.71 was observed for sample with 5% GGBFS and 20% CW at 200 kPa of normal stress, as the sample exhibited the highest peak shear stress value of 193.05 kPa, after 28 days of specimen curing.
6. These results are also supported by SEM micrographs and EDS spectra of stabilised specimen which showed bentonite and slag particles occupying voids and cracks in construction waste particles, which may contribute to better interlocking mechanism in the specimen particle matrix. Alkali oxides (Na_2O, MgO, CaO and K_2O), silica (SiO_2) and metallic oxides (TiO_2, Fe_2O_3 and Al_2O_3) were commonly found the composite specimens inducted by both bentonite and the two stabilisers. *X*-ray diffraction spectra suggested that the specimen curing might have resulted in hydration of CaO to produce $Ca(OH)_2$ from pozzolanic reaction of GGBFS. This can be attributed to the occurrence of higher cohesion and shear stress values of the stabilised samples with the progression of the stabiliser proportions and curing periods.

ACKNOWLEDGEMENTS

The authors acknowledge the use of Curtin University's Microscopy and Microanalysis Facility, whose instrumentation has been partially funded by the University, State and Commonwealth Governments.

REFERENCES

Abdelrahman, G.E., Mohamed, H.K., and Ahmed, H.M. (2013). "New replacement formations on expansive soils using recycled EPS beads." *Proceedings of the 18th International Conference on Soil Mechanics and Geotechnical Engineering*, Paris 2013, 3167–3170.

Amiralian, S., Budihardjo, M.A., Chegenizadeh, A., and Nikraz, H. (2015). "Study of scale effect on strength characteristic of stabilised composite with sewage sludge—Part B: Critical investigation." *Construction and Building Materials*, **80**, 346–350. doi: http://dx.doi.org/10.1016/j.conbuildmat.2015. 01.070.

Australasian (Iron & Steel) Slag Association (2013). *Quick Reference Guide 1 in Roads Guide Supplement on General Applications*. Wollongong: Australasian (Iron & Steel) Slag Association.

Barnett, S.J., Soutsos, M.N., Millard, S.G., and Bungey, J.H. (2006). "Strength development of mortars containing ground granulated blast-furnace slag: Effect of curing temperature and determination of apparent activation energies." *Cement and Concrete Research*, **36**(3), 434–440. doi: http://dx.doi.org/10.1016/j.cemconres.2005.11.002.

Budihardjo, M.A., Chegenizadeh, A., and Nikraz, H. (2015a). "Application of wood to sand-slag and its effect on soil strength." *Procedia Engineering*, **102**, 640–646. doi: http://dx.doi.org/10.1016/j.proeng.2015.01.155.

Budihardjo, M.A., Chegenizadeh, A., and Nikraz, H. (2015b). "Investigation of the strength of carbon-sand mixture." *Procedia Engineering*, **102**, 634–639. doi: http://dx.doi.org/10.1016/j.proeng.2015.01.153.

Deer, W.A., Howie, R.A., and Zussman, J. (2013). *An Introduction to the Rock-Forming Minerals*. 3rd ed. London: Mineralogical Society of Great Britain & Ireland.

Fredericci, C., Zanotto, E.D., and Ziemath, E.C. (2000). "Crystallization mechanism and properties of a blast furnace slag glass." *Journal of Non-Crystalline Solids*, **273**(1), 64–75.

Fredlund, D.G. (2006). "Unsaturated soil mechanics in engineering practice." *Journal of Geotechnical and Geoenvironmental Engineering*, **132**(3), 286–321.

Gardner, L.J., Bernal, S.A., Walling, S.A., Corkhill, C.L., Provis, J.L., and Hyatt, N.C. (2015). "Characterisation of magnesium potassium phosphate cements blended with fly ash and ground granulated blast furnace slag." *Cement and Concrete Research*, **74**(0), 78–87. doi: http://dx.doi.org/10. 1016/j.cemconres.2015.01.015.

Hasan, U., Chegenizadeh, A., Budihardjo, M.A., and Nikraz, H. (2015) "A review of the stabilisation techniques on expansive soils." *Australian Journal of Basic & Applied Sciences*, **9**(7), 541–548.

Hasan, U., Chegenizadeh, A., Budihardjo, M.A., and Nikraz, H. (2016). "Experimental evaluation of construction waste and ground granulated blast furnace slag as alternative soil stabilisers." *Geotechnical and Geological Engineering*, 1–16. http://doi.org/10.1007/s10706-016-9983-z.

Karnland, O. (2010). *Chemical and Mineralogical Characterization of the Bentonite Buffer for the Acceptance Control Procedure in a KBS-3 Repository*. Swedish Nuclear Fuel and Waste Management Co., Stockholm (Sweden).

Karunarathne, A., Gad, E.F., Sivanerupan, S., and Wilson, J.L. (2012). "Review of residential footing design on expansive soil in Australia." in *From Materials to Structures: Advancement through Innovation*, 575–580, CRC Press.

McGrath, T., White, J.F., and Downey, J.P. (2014). "Experimental determination of density in molten lime silicate slags as a function of temperature and composition." Mineral Processing and Extractive Metallurgy (Trans. Inst. Min Metall. C), **123**(3), 178–183.

Murthy, I.N., Babu Arun, N., and Rao Babu, J. (2014). "Comparative studies on microstructure and mechanical properties of granulated blast furnace slag and fly ash reinforced AA 2024 composites." *Journal of Minerals and Materials Characterization and Engineering*, **2**, 319–333. http://dx.doi.org/10.4236/jmmce.2014.24037.

Nidzam, R.M. and Kinuthia, J.M. (2010). "Sustainable soil stabilisation with blastfurnace slag–a review." *Proceedings of the ICE-Construction Materials*, **163**(3), 157–165.

Van Oss, H.G. (2003). *Slag-Iron and Steel*. United States: US Geological Survey Minerals Yearbook.

Ouf, A.R.M.E.-S. (2001). *Stabilisation of Clay Subgrade Soils Using Ground Granulated Blastfurnace Slag*, University of Leeds, Leeds, UK.

Proctor, D.M., Fehling, K.A., Shay, E.C., Wittenborn, J.L., Green, J.J., Avent, C., Bigham, R.D., Connolly, M., Lee, B., and Shepker, T.O. (2000). "Physical and chemical characteristics of blast furnace, basic oxygen furnace, and electric arc furnace steel industry slags." *Environmental Science & Technology*, **34**(8), 1576–1582.

Standards A. (2003). *Methods of Testings Soil for Engineering Purposes: Method 5.1.1: Soil Compaction and Density Tests- Determination of the Dry Density/Moisture Content Relation of a Soil Using Standard Compactive Effort*. AS 1289.5.1.1–2003.

Standards A. AS 1289.6.2.2 (1998). *Methods of Testing Soils for Engineering Purposes-Soil Strength and Consolidation Tests-Determination of the Shear Strength of a Soil-Direct Shear Test Using a Shear Box*.

Venkatramaiah, C. (2006). *Geotechnical Engineering*: New Age International.